

# UPLC and ESI-MS analysis of metabolites of *Rauvolfia tetraphylla* L. and their spatial localization using desorption electrospray ionization (DESI) mass spectrometric imaging



P. Mohana Kumara<sup>a,c,\*\*</sup>, R. Uma Shaanker<sup>b</sup>, T. Pradeep<sup>a,\*</sup>

<sup>a</sup> DST Unit of Nanoscience and Thematic Unit of Excellence, Department of Chemistry, Indian Institute of Technology Madras, Chennai, 600036, India

<sup>b</sup> School of Ecology and Conservation, Department of Crop Physiology, University of Agricultural Sciences, GKVK, Bengaluru, 560065, India

<sup>c</sup> Center for Ayurveda Biology and Holistic Nutrition, The University of Trans-Disciplinary Health Sciences and Technology (TDU), Bengaluru, 560064, India

## ARTICLE INFO

### Keywords:

*Rauvolfia tetraphylla*  
Apocynaceae  
Indole alkaloids  
DESI-MS  
Ajmalicine  
Reserpine  
Yohimbine

## ABSTRACT

*Rauvolfia tetraphylla* L. (family Apocynaceae), often referred to as the wild snakeroot plant, is an important medicinal plant and produces a number of indole alkaloids in its seeds and roots. The plant is often used as a substitute for *Rauvolfia serpentina* (L.) Benth. ex Kurz known commonly as the Indian snakeroot plant or sarphagandha in the preparation of Ayurvedic formulations for a range of diseases including hypertension. In this study, we examine the spatial localization of the various indole alkaloids in developing fruits and plants of *R. tetraphylla* using desorption electrospray ionization mass spectrometry imaging (DESI-MSI). A semi-quantitative analysis of the various indole alkaloids was performed using UPLC-ESI/MS. DESI-MS images showed that the distribution of ajmalicine, yohimbine, demethyl serpentine and mitoridine are largely localized in the fruit coat while that for ajmaline is restricted to mesocarp of the fruit. At a whole plant level, the ESI-MS intensities of many of the ions were highest in the roots and lesser in the shoot region. Within the root tissue, except sarpagine and ajmalicine, all other indole alkaloids occurred in the epidermal and cortex tissues. In leaves, only serpentine, ajmalicine, reserpiline and yohimbine were present. Serpentine was restricted to the petiolar region of leaves. Principal component analysis based on the presence of the indole alkaloids, clearly separated the four tissues (stem, leaves, root and fruits) into distinct clusters. In summary, the DESI-MSI results indicated a clear tissue localization of the various indole alkaloids, in fruits, leaves and roots of *R. tetraphylla*. While it is not clear of how such localization is attained, we discuss the possible pathways of indole alkaloid biosynthesis and translocation during fruit and seedling development in *R. tetraphylla*. We also briefly discuss the functional significance of the spatial patterns in distribution of metabolites.

## 1. Introduction

*Rauvolfia tetraphylla* L. (Family Apocynaceae) (Fig. 1a) is an economically important medicinal plant, often used as a substitute for its conspecific plant, *Rauvolfia serpentina* (L.) Benth. ex Kurz commonly referred to as the Indian snakeroot plant or sarphaganda (Gupta et al., 2012). The latex of both species of plants are used in a variety of cures in folk medicine and several indigenous or traditional medicine systems (Gupta et al., 2012). The white latex is used as emetic, cathartic and expectorant for treating dropsy (Gupta et al., 2012; Kaushik et al., 2013). Both the species of *Rauvolfia* produce a variety of monoterpene indole alkaloids (MIAs) such as reserpine, serpentine,

deserpidine, ajmaline, ajmalicine, yohimbine that have been reported to have important pharmaceutical and biological activities. All these compounds originate from strictosidine (Fig. 2), formed by the condensation of tryptamine with secologanin (Hagel et al., 2008; Pan et al., 2015). Little is known about the downstream biosynthetic pathway of these compounds from strictosidine (Fig. 2) (Faisal et al., 2005).

Considering the importance of many of the monoterpene indole alkaloids (MIAs) in pharmaceutical applications, a number of studies have explored to unravel the pathway genes involved in the biosynthesis of these compounds. Using an integrated transcriptomics and proteomics approach for gene discovery, Miettinen et al. (2014) discovered the last four missing steps of the (seco)iridoid biosynthesis pathway in

\* Corresponding author.

\*\* Corresponding author. DST Unit of Nanoscience and Thematic Unit of Excellence, Department of Chemistry, Indian Institute of Technology Madras, Chennai, 600036, India.

E-mail addresses: [monapatelpgatti@gmail.com](mailto:monapatelpgatti@gmail.com) (P. Mohana Kumara), [pradeep@iitm.ac.in](mailto:pradeep@iitm.ac.in) (T. Pradeep).

<https://doi.org/10.1016/j.phytochem.2018.11.009>

Received 4 June 2018; Received in revised form 15 November 2018; Accepted 16 November 2018

Available online 17 December 2018

0031-9422/ © 2018 Elsevier Ltd. All rights reserved.

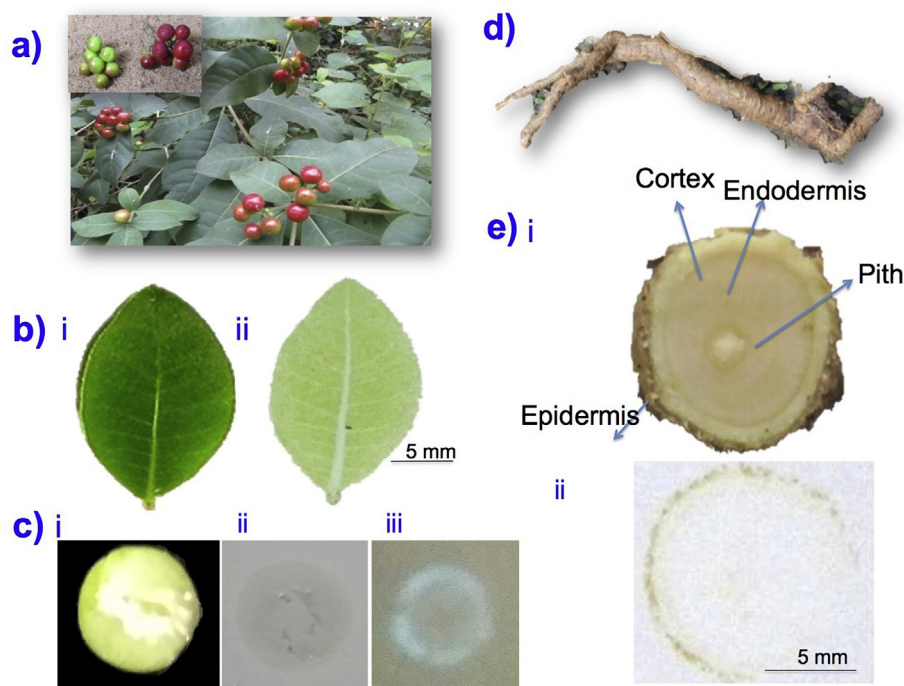


Fig. 1. a) Fruit bearing *Rauvolfia tetraphylla* plant. Insert in shows the different stages of fruit b) leaf and its TLC imprint, c) Fruit cross section (i) and its TLC imprint (ii) TLC imprint photo taken with UV light (iii) d) Root and e) Root cross section (i) and its TLC imprint (ii).

*Catharanthus roseus*. More recently, the entire MIA pathway up to strictosidine was engineered in *Nicotiana benthamiana* by heterologous expression of newly identified genes in combination with the previously known biosynthesis genes (Miettinen et al., 2014). Interestingly the biosynthetic pathways of many plant specialised metabolites often involve multiple cell types that are biochemically and morphologically distinct (Hagel et al., 2008; Pan et al., 2015). *In situ* RNA hybridization and immuno-cytochemical studies have shown the localization of MIA pathway enzymes to a number of cell types (St-Pierre et al., 1999). For example, studies in *C. roseus* have shown that secoiridoid metabolism begins in phloem-associated parenchyma cells (IPAP) cells and that loganic acid produced in IPAP cells is transferred to epidermal cells (ECs). Further synthesis involving secologanin and tryptamine occurs in the ECs. Finally, a MIA intermediate, deacetoxyvindoline, moves to the idioblast cells (ICs) and laticifer cells (LCs) and MIAs begin to accumulate in the vacuole of these cells (St-Pierre et al., 1999; Mahroug et al., 2006; Dug e de Bernonville et al., 2015; Burlat et al., 2004).

In a more recent study on a Mediterranean plant, *Thapsia garganica* (dicot, Apiaceae), using MALDI MSI, it was shown that the metabolite, thapsigargin was stored in the secretory ducts in the roots. Transcripts of *TgTPS2* (epikunzeol synthase) and *TgCYP76AE2* in roots were found only in the epithelial cells lining these secretory ducts (Andersen et al., 2017). Similarly, in *Vitex agnuscastus* L, MALDI-MSI analysis showed that the diterpenoids were localized in trichomes on the surface of fruit and leaves. Analysis of a trichome-specific transcriptome database, coupled with expression studies, identified seven candidate genes involved in diterpenoid biosynthesis (Heskes et al., 2018; Boughton et al., 2016).

Unraveling the localization of pathway gene expression and their products or metabolites can profoundly help in understanding, both the regulatory and functional basis of metabolite synthesis in plants (Miettinen et al., 2014). While traditionally, studies have relied on techniques such as *in situ* RNA hybridization and immuno-cytochemical studies, in recent years there has been increasing attempts to use mass spectrometry imaging techniques for localizing plant metabolites. These techniques, such as MALDI-MSI or DESI-MSI are rapid, easy to use and have been used in a number of studies to understand the spatial

context of metabolite accumulation and localization (Bjarnholt et al., 2014; Lee et al., 2012; Ifa et al., 2011; Korte et al., 2012; Hemalatha and Pradeep, 2013; Kueger et al., 2012; Boughton et al., 2016; Andersen et al., 2017; Zifkin et al., 2012). Coupled with tissue-based transcriptomic analysis, the technique can potentially be used in unraveling biosynthetic pathway genes responsible for the synthesis and accumulation of specialised metabolites (Bjarnholt et al., 2014; Zifkin et al., 2012; Andersen et al., 2017).

In this study, using a DESI-MSI approach, we have developed a spatially explicit map of the indole alkaloids in developing fruits and plants of *R. tetraphylla*. We rationalize the results based on both the functional significance of such patterns as well as the possible metabolic regulatory processes that might have resulted in these patterns.

## 2. Results and discussion

ESI MS analysis of the different parts (root, stem, leaf and fruits: Fig. 1) of *R. tetraphylla* showed the presence of prominent metabolites in the range of  $m/z$  300–611 (Table 1). Among the different tissues, by far the roots contained relatively large number of indole alkaloids compared to the stem, leaves and fruits (Fig. S1). Structural characterization of these indole alkaloids were done by both accurate mass measurement and mass fragmentation analysis (Fig. S2) (Smith et al., 2005). Mass fragmentation analysis was done mainly by comparing the observed fragment ions with those retrieved from earlier publications (Fig. S2). Where not available, the patterns were annotated using the fragments core structural features (Supplementary information; Fig. S2). A list of  $m/z$  values of the parent and fragment ions and their chemical formulae are given in Table 1. Based on these masses, the identity and the spatial location of the compounds were established in different parts of the fruit and plant using DESI-MS imaging facility. Principal component analysis (PCA) based on the presence of MIAs clearly separated the four tissues (stem, leaves, root and fruits) in to distinct clusters (Fig. S2). The first and second PC axis respectively explained 66.5% and 30.5% of the variance. The eigenvector contributions for the two axes are: PC1 Leaf-L1 (2.0994) L2 (4.827) L3 (4.827) and PC2 (L1 3.990, Root-R2 0.29, R3- 0.217) (Fig. S3).

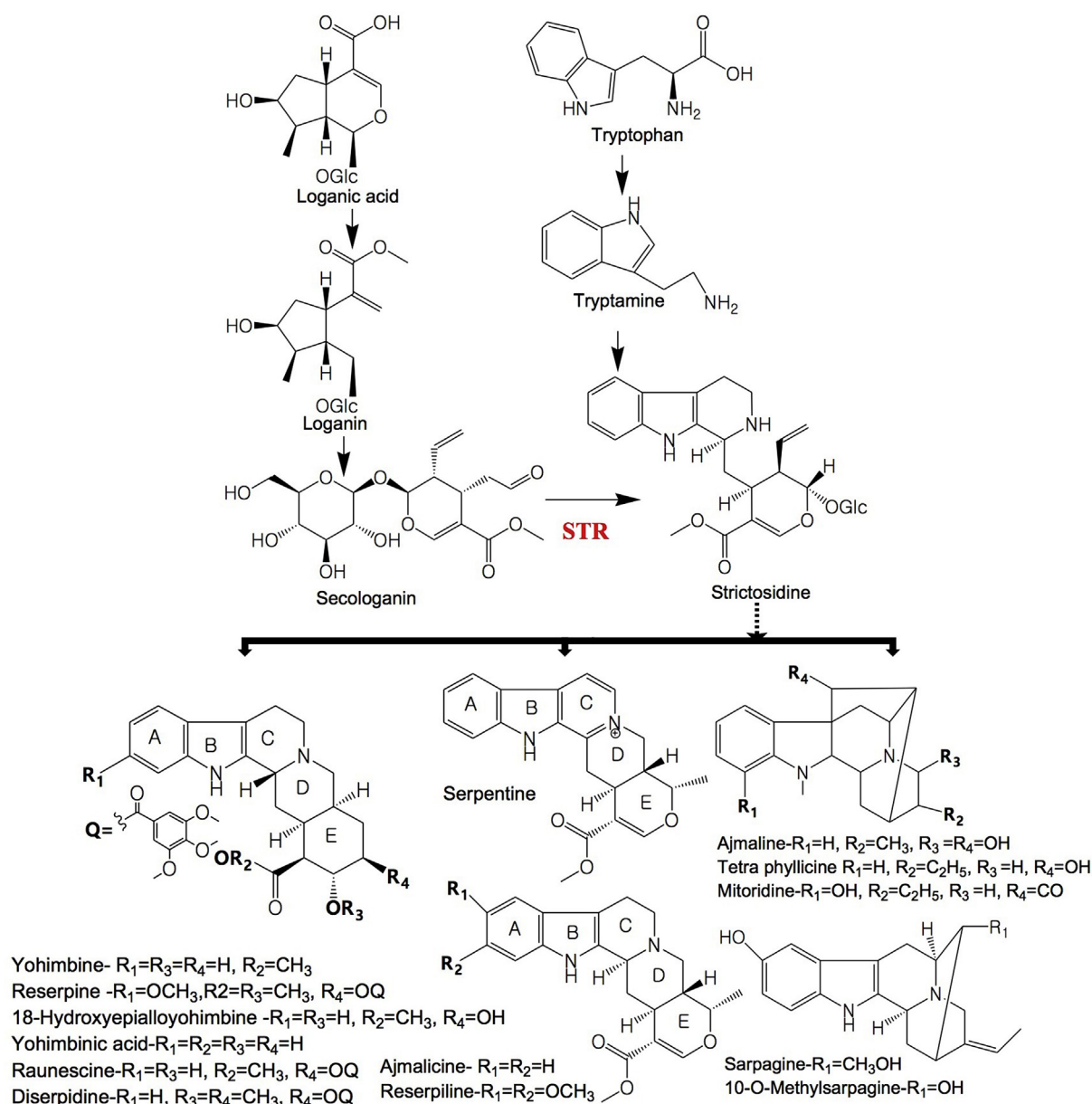


Fig. 2. Pathway of monoterpenoid indole alkaloid biosynthesis. Strictosidine synthase (STR) is a key gene responsible for the biosynthesis of strictosidine. Strictosidine is a major precursor for the biosynthesis of a diversity of MIAs in *Rauvolfia tetraphylla*.

### 2.1. MIAs during fruit development

The spatial locations of different MIAs in cross section of developing fruits were established using DESI-MS. Among the various indole alkaloids, prominent were mitoridine, ajmaline, demethyl serpentine, ajmalicine and yohimbine (Fig. 3). The molecular ion intensities were higher in early stage fruits compared to mature fruit. The alkaloids, mitoridine, 12-methoxyvellosimine, demethyl serpentine, ajmalicine and yohimbine were restricted to the fruit coat (exocarp), while ajmaline was largely restricted to mesocarp of the fruit (Fig. 3). Demethyl serpentine was detected only in fruits and not in other parts of the plant.

### 2.2. MIAs in root and shoot

Cross-sections of root and shoot of the plant showed distinct spatial distribution patterns of the various ions. In roots, most of the indole alkaloids were present and showed tissue specific localization.

Tetrahyllicine, raunescine and deserpidine were present only in epidermis; mitoridine and ajmalicine were present in cortex while reserpine was restricted to the pith region only. Sarpagine, 10-O-methylsarpagine, ajmaline, serpentine, yohimbine and 18-hydroxy-yohimbine were present in higher abundance in epidermis and pith region. Stem contained, sarpagine, ajmaline, serpentine, ajmalicine, yohimbine and 18-hydroxy-yohimbine with a localization pattern similar to that in the root (Fig. 4).

### 2.3. MIAs in leaves

In leaves, only serpentine, ajmalicine, reserpiline and yohimbine were found. Specifically, serpentine was found only in the leaf petiole while the other metabolites were abundant in the leaf blade (Fig. 5).

Intensities of many of these metabolites were highest in the roots upwards to the collar region, representing the transition from the root to the shoot (Figs. 3–5, Fig. S5). For example, reserpine content on dry weight basis, was highest in the main roots ( $0.50\% \pm 0.10$ ) and lateral

**Table 1**  
 Details of  $m/z$  values of the ions, fragment ions and chemical formulae of monoterpene alkaloids identified in *Rauwolfia tetraphylla*.

Serial number	Metabolite	Ion type	Exact mass (calculated)	$m/z$ obtained from ESI MS (Orbitrap)	Error (ppm)	Chemical Formula	Mass fragments <sup>a</sup>	Metabolite tissue localization		
								Root/stem	Leaves	Fruit
1	Strictosidine	[M+H] <sup>+</sup>	531.2337	531.2337	0	C <sub>27</sub> H <sub>35</sub> N <sub>2</sub> O <sub>9</sub>	514, 352, 334, 320, 302, 282, 251, 222, 223, 144			
<b>Reserpine type of alkaloids</b>										
2	Yohimbine	[M+H] <sup>+</sup>	385.2016	355.2007	-2.5	C <sub>21</sub> H <sub>27</sub> N <sub>2</sub> O <sub>3</sub>	337, 323, 224, 212, 194, 144	Epidermis and pith	Leaf blade	-
3	Deserpidine	[M+H] <sup>+</sup>	579.2701	579.2698	-0.5	C <sub>32</sub> H <sub>39</sub> N <sub>2</sub> O <sub>8</sub>	547, 448, 367, 335, 195, 144	Epidermis	-	-
4	Reserpine	[M+H] <sup>+</sup>	609.2807	609.2802	-0.8	C <sub>33</sub> H <sub>41</sub> N <sub>2</sub> O <sub>9</sub>	577, 448, 436, 397, 365, 336, 236, 224, 195	Pith	-	-
5	18-Hydroxyepialloyohimbine	[M+H] <sup>+</sup>	371.1965	371.1961	-1.0	C <sub>21</sub> H <sub>27</sub> N <sub>2</sub> O <sub>4</sub>	353, 339, 240, 2281, 58, 223, 144	Epidermis and pith	-	-
6	Yohimbic acid	[M+H] <sup>+</sup>	341.1865	341.1862	-0.8	C <sub>20</sub> H <sub>25</sub> N <sub>2</sub> O <sub>3</sub>	32, 32, 1, 19, 61, 58, 144	Epidermis and pith	-	-
7	Raunescine	[M+H] <sup>+</sup>	565.2544	565.2542	-0.3	C <sub>31</sub> H <sub>35</sub> N <sub>2</sub> O <sub>8</sub>	547, 448, 353, 321, 195, 144	Epidermis	-	-
<b>Ajmalicine type of alkaloids</b>										
8	Ajmalicine	[M+H] <sup>+</sup>	353.186	353.1851	-2.5	C <sub>21</sub> H <sub>25</sub> N <sub>2</sub> O <sub>3</sub>	321, 293, 210, 222, 144	Cortex	Leaf blade	Outer part
9	Reserpiline	[M+H] <sup>+</sup>	413.2071	413.2068	-0.7	C <sub>23</sub> H <sub>29</sub> N <sub>2</sub> O <sub>5</sub>	381, 222, 204, 144	-	Leaf blade	-
<b>Ajmaline type of alkaloids</b>										
10	Ajmaline	[M+H] <sup>+</sup>	327.2067	327.2063	-1.2	C <sub>20</sub> H <sub>27</sub> N <sub>2</sub> O <sub>2</sub>	309, 238, 210, 194, 182, 158, 144	Epidermis and pith	-	Endosperm
11	Tetrahyllicine	[M+H] <sup>+</sup>	309.1961	309.1957	-1.3	C <sub>20</sub> H <sub>25</sub> N <sub>2</sub> O	291, 238, 182, 158, 144	Epidermis	-	-
12	Sarpagine	[M+H] <sup>+</sup>	311.176	311.175	-3.2	C <sub>19</sub> H <sub>23</sub> N <sub>2</sub> O <sub>2</sub>	293, 276, 165, 145, 138	Epidermis and pith	-	-
13	Mitoridine	[M+H] <sup>+</sup>	323.176	323.1749	-3.4	C <sub>20</sub> H <sub>23</sub> N <sub>2</sub> O <sub>2</sub>	305, 291, 279, 263, 144	Cortex	-	Outer part
14	10-O-Methylsarpagine	[M+H] <sup>+</sup>	325.1911	325.1907	-3.4	C <sub>20</sub> H <sub>25</sub> N <sub>2</sub> O <sub>2</sub>	307, 293, 160, 144	Epidermis and pith	-	-
<b>Others</b>										
15	Serpentine	[M+H] <sup>+</sup>	349.1547	349.1537	-2.8	C <sub>21</sub> H <sub>21</sub> N <sub>2</sub> O <sub>3</sub>	317, 293, 277, 263, 235	Epidermis and pith	Leaf petiole	-
16	Demethyl serpentine	[M+H] <sup>+</sup>	335.1396	335.1382	-4.1	C <sub>20</sub> H <sub>19</sub> N <sub>2</sub> O <sub>3</sub>	317, 293, 277, 263, 235	-	-	Outer part

- Below detection threshold.

<sup>a</sup> The mass fragments used to infer the chemical identities of the various compounds are based on published literature provided for each of the alkaloids in the supplementary information.

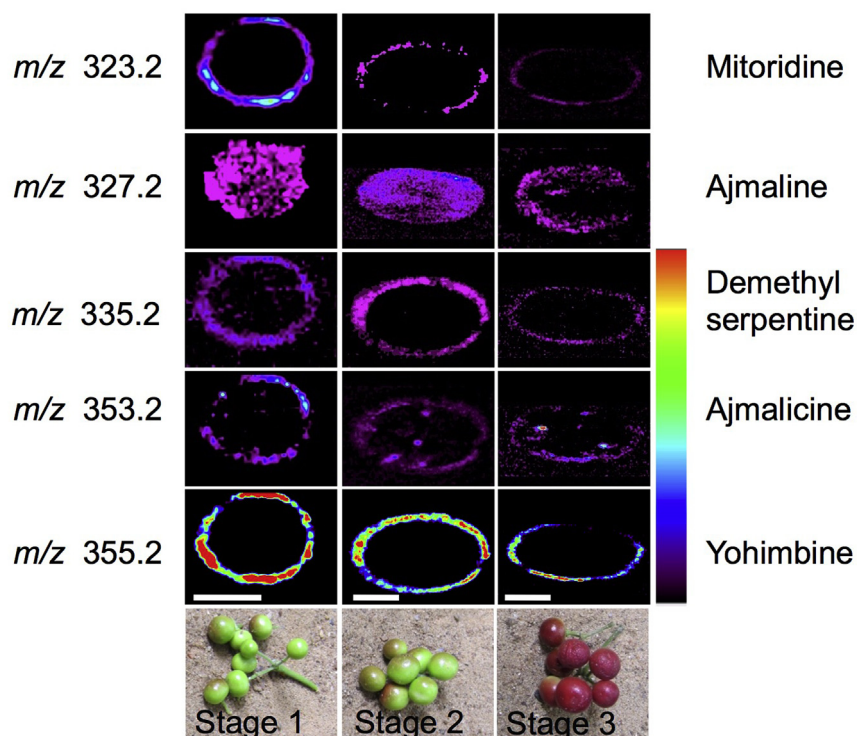


Fig. 3. DESI MS images showing the distribution of indole alkaloids in fruit sections of *R. tetraphylla*. Scale bars correspond to 5 mm and apply to all the images of a row.

roots ( $0.44\% \pm 0.09$ ), followed by stem ( $0.31\% \pm 0.09$ ), and least in fruits ( $0.02\% \pm 0.02$ ) and absent in leaves (Fig. 6).

In summary, our results show that the MIAs in *R. tetraphylla* exhibit a distinct localization patterns, both, across and within different tissues (Figs. 3 and 4). For example, while roots contained most of the MIAs, the stems contained only sarpagine, ajmaline, serpentine, ajmalicine, yohimbine and 18-hydroxy-yohimbine. Similarly, the leaves had only serpentine, ajmalicine, reserpiline and yohimbine. Within each tissue as well, there were distinct patterns of occurrence. In fruits, several of the MIAs were restricted to the fruit coat, while others were restricted to the mesocarp. Similarly, within roots, there was a clear spatial separation of several of the MIA between the epidermal and cortex tissues. These results add to the now growing literature that suggests there could be spatial patterning of occurrence of specialised metabolites, across and within tissues (Dueñas et al., 2017; Bhandari et al., 2015; Mohana Kumara et al., 2016; Sturtevant et al., 2017). These are now increasingly becoming evident, especially through studies, involving non-invasive, imaging analysis including MALDI MSI and DESI MSI (Bjarnholt et al., 2014; Lee et al., 2012; Ifa et al., 2011; Korte et al., 2012; Hemalatha and Pradeep, 2013; Kueger et al., 2012; Dopstadt et al., 2017; Woodfield et al., 2017). The spatial patterning of MIAs also raises interesting questions, both proximate and ultimate, of such occurrence. Proximately, the patterns are best explained by studying the underlying gene expression patterns, and examining, if there is indeed any spatial correlation between the expression and the occurrence. A few studies have attempted to examine such correlation by analyzing cell and tissue specific transcriptome data. For example, in flaxseed (*Linum usitatissimum*), expression of the key genes involved in the synthesis of pinosresinol and the subsequent downstream pathway intermediate were correlated with the spatial distribution of metabolite (Dalisay et al., 2015). Similarly, in highbush blueberry (*Vaccinium corymbosum*), occurrence of major classes of flavonoids was correlated to the transcript abundance. Proanthocyanidins (PAs) and corresponding transcripts encoding anthocyanidin reductase and leucoanthocyanidin reductase were mostly concentrated in young fruits

and localized predominantly to the inner fruit tissue containing the seeds and placentae (Zifkin et al., 2012). In *Calotropis procera*, tissue specific expression analysis of 30 putative transcripts involved in terpenoid, steroid and cardenolide pathways were correlated with metabolite and transcript accumulation (Pandey et al., 2016). In tea leaves, the expression patterns of genes in C2-2-1 and C2-2-2-1 groups were found to be probably responsible for the development-dependent accumulation of phenolic compounds in the leaves (Jiang et al., 2013). In *Sorghum bicolor*, during accumulation was reported to be correlated with transcript abundance of genes involved in biosynthesis of cyanogenic glycosides (Nielsen et al., 2016). It would be interesting to examine such association between the spatial distribution of the metabolites in tissues with the corresponding gene expression in *R. tetraphylla* as well. Where such correlation between spatial localization and gene expression is not evident, it is likely that the spatial patterns could be due to a disconnect between the sites of synthesis and sites of accumulation of the metabolites. For example, in pea and carrot, cytokinins biosynthesized in cambium of the root is finally exported to the shoot (Chen et al., 1985).

While the above studies may help explain the proximate basis of spatial patterning of metabolites, it is also interesting to examine, the ultimate functional significance of such patterning. One of the earliest studies is due to Berenbaum (1995) who proposed the concept of apparency in the synthesis and accumulation of specialised metabolites by plant tissue. According to this theory, plants bet-hedge on deploying defense responses and investing carbon to synthesizing specialised metabolites. Thus, instead of uniformly investing in synthesis and accumulation of specialised metabolites in all leaves, plants may accumulate the compound in only a proportion of the leaves and within a leaf, only in some parts of the leaf (Hansen et al., 2016). In *R. tetraphylla*, it is interesting to note that ajmaline is specifically distributed in the mesocarp of the fruit and increases through the fruit developmental phase. Ajmaline is a potent inhibitor of  $\text{Na}^+/\text{K}^+$  channel (Kiesecker et al., 2004) and it is likely that the accumulation pattern in the mesocarp could help defend the fruit from insect herbivores. On the

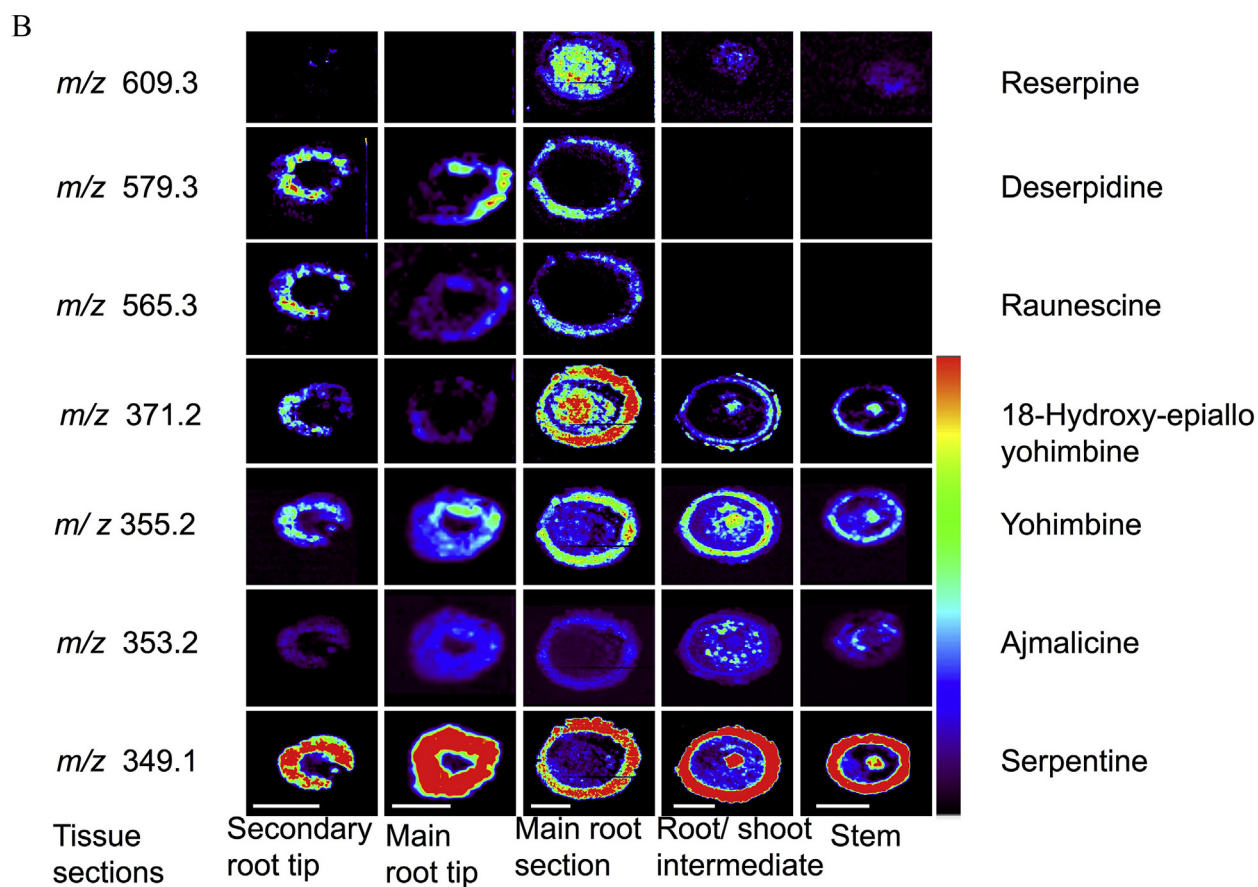
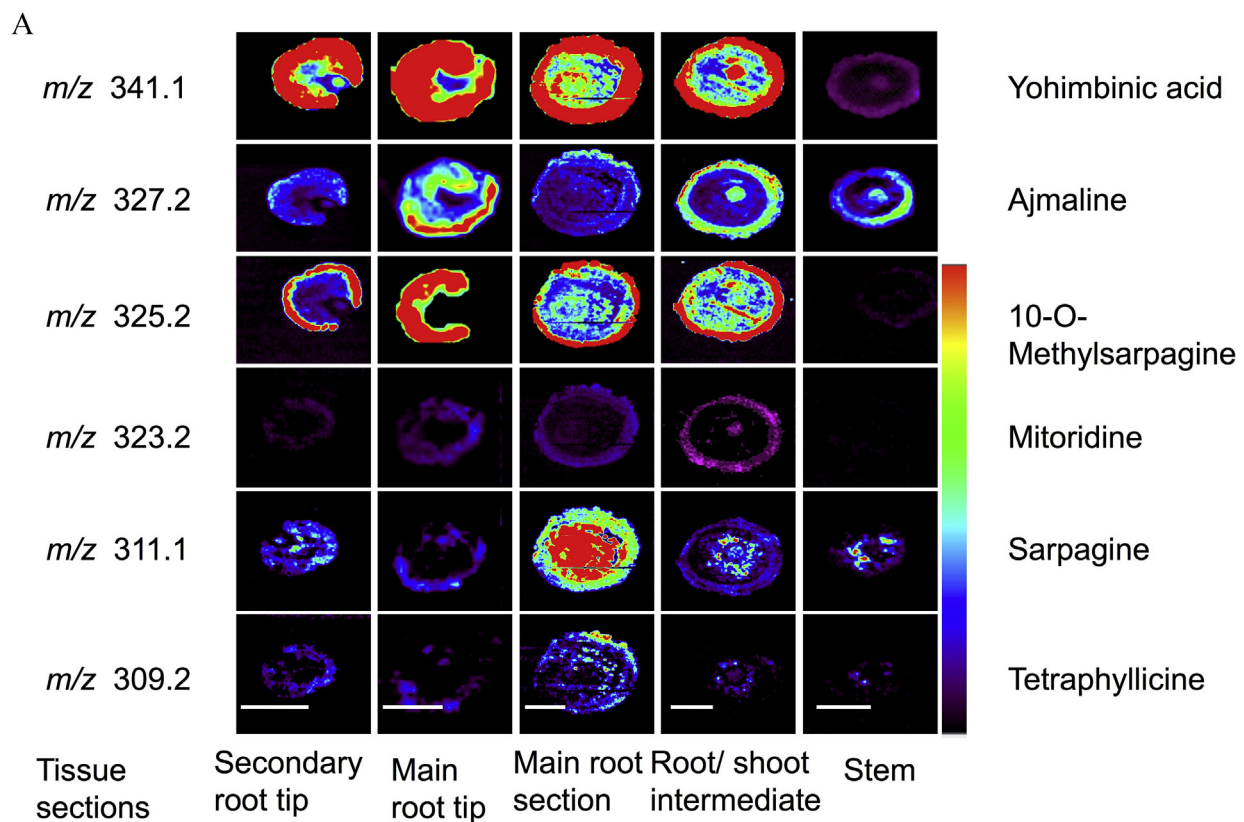


Fig. 4. DESI MS images showing the indole alkaloid distribution in root and stem sections of *R. tetraphylla*. Scale bars correspond to 5 mm and apply to all the images of a row.

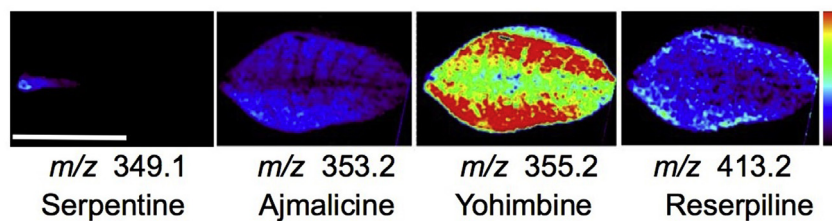


Fig. 5. DESI MS images showing the indole alkaloid distribution in leaf of *R. tetraphylla*. Scale bars correspond to 5 mm and apply to all the images of a row.

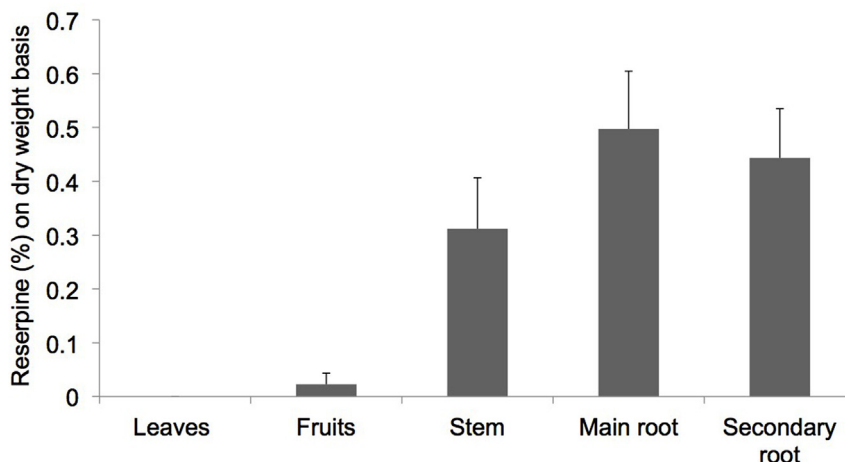


Fig. 6. Reserpine content (on dry weight basis) in different parts of *Rauvolfia tetraphylla* plant. Error bars indicates standard deviation.

other hand, ion intensities of many other compounds such as mitrodine, yohimbine that was located in the fruit epidermis decreased with fruit ripening. The functional significance of many of these compounds is unknown, though some of them might serve as intermediates of biosynthesis of indole alkaloids. Yohimbine is an alpha adrenoreceptor inhibitor and could possibly also function in defense. Sarpagine, an ajmaline type monoterpene indole alkaloid, is a  $\text{Na}^+$  channel blocker and is concentrated in the cortex and pith of the root. Reserpine, also abundant in the main root cortex, is a monoamine transport blocker (Mahata et al., 1996). Ajmalicine, an andregnic receptor antagonist, is concentrated in the epidermis and cortex. The functional significance of most of these compounds are yet unknown and clearly more research is required to unravel their significance to plant growth and defense.

Like other terpene alkaloids, the synthesis of MIA begins with the condensation of tryptamine and secologanin to yield strictosidine. Strictosidine is converted into 4,21-dehydrogeissoschizine and thereafter through cyclization and reduction, ajmalicine is formed (KEGG pathway). However, in our study, we failed to recover the primary precursors of the different MIAs. An earlier study (Yamamoto et al., 2016) employing nano-DESI was successful in locating some of the precursors, such as strictosidine, indicating perhaps the need for high-resolution imaging to capture such molecules. It is also likely that our failure to spatially detect them could be due to them not being readily ionized as well as because of their inherently poor stability.

It is now well acknowledged that the primary site of synthesis of the MIAs is the root (Schlutenhofer et al., 2014; O'Connor and Maresh, 2006) and from there perhaps, a few are transported elsewhere in the plant (El-Sayed and Verpoorte, 2007; Liu et al., 2017; Pathania and Acharya, 2016). We have made a preliminary attempt to explore if there exist a tacit relationship between the spatial patterning of the specialised metabolites and their biosynthetic pathway (Figs. 7 and 8). Understandably, the root sections have the largest diversity of MIAs, perhaps representing the pathway intermediaries as well. However there is a clear narrowing of such diversity in the root:stem collar region and thereafter in the stem region, only to be partially restored in

the leaf and fruits. That there is an active transport is supported by the fact that transporters of ajmalicine and other MIAs have been reported (Liu et al., 2017; Zhu et al., 2015; Pathania and Acharya, 2016; Yu and De Luca, 2013).

In conclusion, the study provides a spatial framework of MIAs in different parts of *R. tetraphylla* plants. These results could serve as valuable inputs for further studies to address, both the proximate causes and the ultimate selective advantage of such patterning. Combined with other omics approaches, including transcriptomics/metabolomics, DESI MS imaging of specialised metabolites can offer exciting opportunities to explore tissue specific, and in some cases, cell specific gene expression to validate the spatial occurrences of metabolites.

### 3. Materials and methods

#### 3.1. Plant material

*R. tetraphylla* plants were raised and maintained at IIT Madras Nursery, Chennai (13.0052° N, 80.2420°E). *R. tetraphylla* produces brightly colored fruits, green during early stage, yellowish to red during maturity and shiny black during fully matured stage. The seeds take approximately 30–50 days to mature. Different plant parts were collected from the two-year-old plant during winter season (19-01-2015). Plant was up rooted, segmented into different parts, namely, root, stem and leaves (Fig. 1). Root and stem were further segmented in four different sections, namely, epidermis, cortex endodermis and pith region respectively (Fig. 1e). Different developmental stages of the fruit were collected from the two-year-old plants.

#### 3.2. ESI-MS/MS, orbitrap analysis and assigning the metabolites

Different sections of the root, shoot, and leaves (corresponding to regions that were used for the imaging) were cut into small pieces and soaked in methanol for 12 h. The solution was filtered and centrifuged at 10,000 rpm for 10 min. The supernatant was analyzed by ESI MS/MS

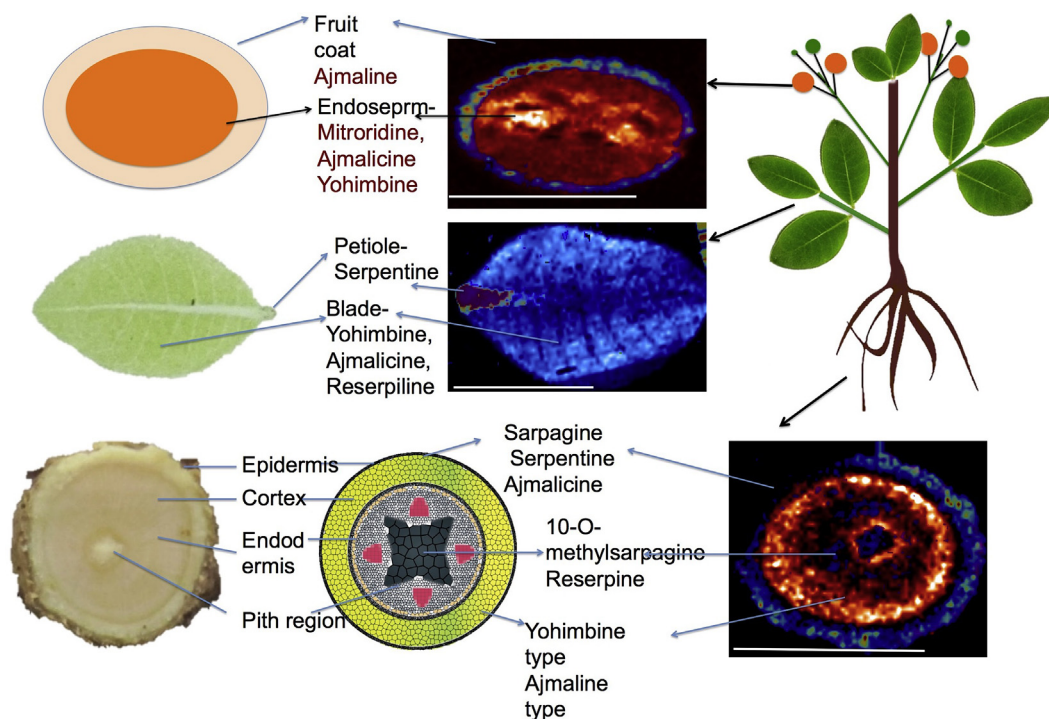


Fig. 7. Superimposed images of root, leaf and fruit sections of *R. tetraphylla* showing the tissue localization of indole alkaloids.

using Thermo Scientific LTQ XL (Thermo Scientific, San Jose, CA, USA) mass spectrometer, and exact mass was analyzed using Thermo Scientific Orbitrap Elite (Thermo Scientific, San Jose, CA, USA) mass spectrometer. The data was acquired in positive ion mode with a spray voltage of 3 kV. Collision induced dissociation (CID) was used for fragmentation of the ions during MS/MS measurements. The identities

of the ions were established based on both, the fragmentation patterns and exact masses of the ions obtained using METLIN and MassBank metabolite database. The mass window tolerance of  $\pm 3$  ppm was used for database search. The MS/MS data was used to infer the compound identity by comparing the fragment ion  $m/z$  with published literature and database. All the spectra were represented in the profile mode.

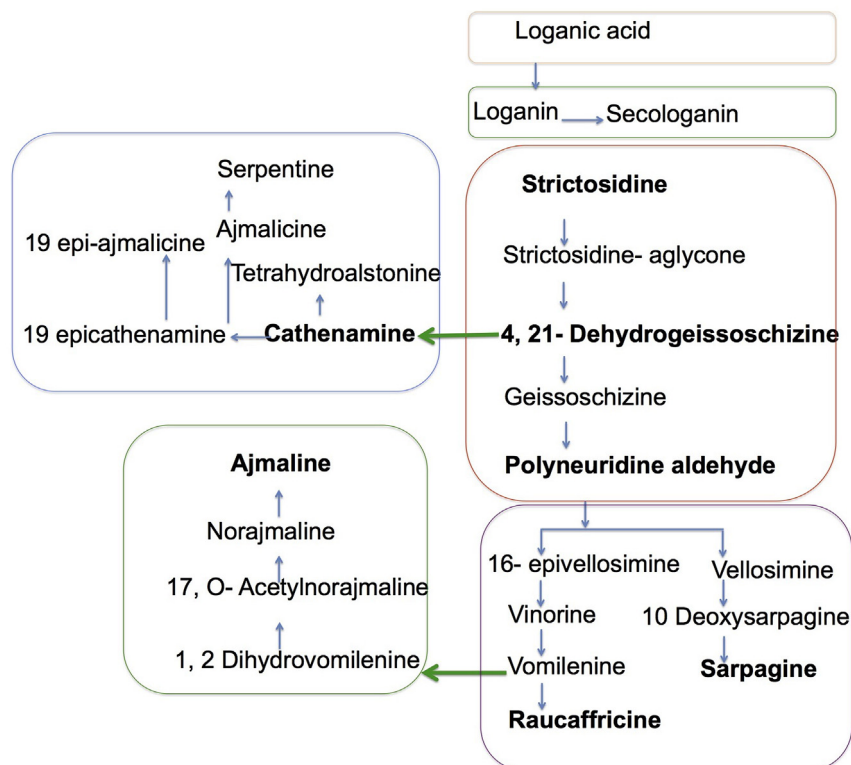


Fig. 8. Schematic illustration of the biosynthesis of monoterpene indole alkaloids (modified from KEGG pathways and Yamamoto et al., 2016).

### 3.3. Extraction and quantification of reserpine using UPLC analysis

Different sections of the root, shoot, and leaves of *R. tetraphylla* were collected from the nursery and oven dried for 3 days at 70 °C (Fig. 1). Tissues were powdered and extracted using 5 mL of methanol (Merck), centrifuged at 10,000 rpm for 5 min and filtered with 0.2 µm filters. Filtered sample (2 µL) was analyzed using UPLC Waters ACQUITY UPLC™ system SYNAPT G2-Si equipped with a binary solvent delivery system, an autosampler, column manager, and a tunable MS detector. Chromatographic separation was performed on a Waters ACQUITY UPLC™ BEH, C18 (130 Å, 1.7 µm, 2.1 mm × 50 mm, 1/pkg) column at 40 ± 5 °C. The mobile phase employed for UPLC analysis consisted of water; methanol (50:50 v/v) in a gradient mode, which was degassed, previously. The flow rate of the mobile phase was kept at 0.50 mL/min and 2 µL of sample solution was injected in each run. The total chromatographic run time was 5 min in resolution mode. The column and autosampler were maintained at 40 ± 5 and 4 ± 5 °C, respectively and pressure of the system was set to 15,000 psi. Care was exercised to ensure that the initial and final volumes of the extract were maintained constant for the sample. Standard curve was developed for the concentration range of 0.125 mg/mL to 1 mg/mL of standard reserpine (Sigma). The best fit ( $R^2 = 0.99$ ) was used in calculating the amount of reserpine in the sample (Fig. S4). All estimates were done on 3 replicates. Semi-quantitative analyses of other indole alkaloids were determined based on the extracted ion chromatogram for the specific ions (Fig. S5).

### 3.4. DESI MS analysis

Plant was uprooted and washed with running tap water and later with distilled water to remove all the debris from the root and other parts (Fig. 1a). Plants were segregated in different parts such as root, stem, leaves and fruits. Stem and roots were cross-sectioned (about 2 mm thick) using surgical blade (Fig. 1e). Fruits were collected at three developmental stages, namely immature (green), mature (green) and ripened (orange to red). Cross sections were made at mid-axis of the fruit and imprinted on flat surface of TLC plate for 10 s to obtain the imprint (TLC Silica gel 60 F<sub>254</sub>, Merck KGaA, Germany). Prior to imprinting, the TLC plates were pre-wetted with methanol and kept on a heating mantle (~70 °C) to obtain molecules present on the cut-end of the sections (Cabral et al., 2013; Mohana Kumara et al., 2015). Young leaves were imprinted on a TLC plate with 2 ton pressure for 15–30 s using a hydraulic pelletizer.

Imaging experiments were conducted using Thermo Scientific LTQ XL (Thermo Scientific, San Jose, CA, USA) mass spectrometer with 2D DESI ion source (Omni Spray Ion Source) from ProSolia, Inc., Indianapolis, IN, USA. The DESI source conditions were as follows; nebulizing gas (dry nitrogen) pressure: 150 psi, spray angle: 60°, tip of spray to surface: 1 mm, tip to inlet distance: 3 mm, spray solvent: methanol, solvent flow rate: 5 µL, spray voltage: 5 kV, and ionization mode: positive (+ve). The image area was chosen according to the sample dimensions and the spatial resolution used was 250 µm × 250 µm. Imaging 1 cm × 1 cm area of tissue sample took approximately 30 min. Imaging time varied with area of the tissue samples. Image files (IMG File) were created using FireFly software from the acquired data and Biomap 3 software was used to process the image files to create images.

### 3.5. Principal component analysis (PCA)

Principal component analysis (PCA) was done based on the exact masses of the compounds ( $m/z$  150–1000 range) recovered from fruits, leaves, and roots to examine if there is a differentiation of the tissues based on their metabolite content. Three representatives mid-point DESI MS spectra corresponding to the different tissues were collected and the masses were extracted for PCA analysis. The analysis was

performed using the statistical software PAST 3.08 (Hammer et al., 2001). The PCA analysis was based on a variance-covariance matrix.

### Conflicts of interest

The authors declare no conflict of interest.

### Acknowledgements

We thank Department of Science and Technology (DST), Government of India for the financial support to carry out this work. P.M.K. thanks IIT Madras, Chennai for a postdoctoral fellowship CY141PF02 and SERB-DST Fast track grant File No SB/YS/LS-361/2013 for financial support.

### Appendix A. Supplementary data

Supplementary data to this article can be found online at <https://doi.org/10.1016/j.phytochem.2018.11.009>.

### References

- Andersen, T.B., Martinez-Swatson, K.A., Rasmussen, S.A., Boughton, B.A., Jørgensen, K., Andersen-Ranberg, J., Nyberg, N., Christensen, S.B., Simonsen, H.T., 2017. Localization and in-vivo characterization of *Thapsia garganica* CYP76AE2 indicates a role in thapsigargin biosynthesis. *Plant Physiol.* 174, 56–72.
- Berenbaum, M.R., 1995. The chemistry of defense: theory and practice. *Proc. Natl. Acad. Sci. U. S. A.* 92, 2–8.
- Bhandari, D.R., Wang, Q., Friedt, W., Spengler, B., Gottwald, S., Rompp, A., 2015. High resolution mass spectrometry imaging of plant tissues: towards a plant metabolite atlas. *Analyst* 140, 7696–7709.
- Bjarnholt, N., Li, B., D'Alvise, J., Janfelt, C., 2014. Mass spectrometry imaging of plant metabolites - principles and possibilities. *Nat. Prod. Rep.* 31, 818–837.
- Boughton, B.A., Thinakaran, D., Sarabia, D., Bacic, A., Roessner, U., 2016. Mass spectrometry imaging for plant biology: a review. *Phytochemistry Rev.* 15, 445–488.
- Burlat, V., Oudin, A., Courtois, M., Rideau, M., St-Pierre, B., 2004. Co-expression of three MEP pathway genes and geraniol 10-hydroxylase in internal phloem parenchyma of *Catharanthus roseus* implicates multicellular translocation of intermediates during the biosynthesis of monoterpene indole alkaloids and isoprenoid-derived primary metabolites. *Plant J.* 38, 131–141.
- Cabral, E., Mirabelli, M., Perez, C., Ifa, D., 2013. Blotting assisted by heating and solvent extraction for DESI-MS imaging. *J. Am. Soc. Mass Spectrom.* 24, 956–965.
- Chen, C.M., Ertl, J.R., Leisner, S.M., Chang, C.C., 1985. Localization of cytokinin biosynthetic sites in pea plants and carrot roots. *Plant Physiol.* 78, 510–513.
- Dalisay, D.S., Kim, K.W., Lee, C., Yang, H., Rübél, O., Bowen, B.P., Davin, L.B., Lewis, N.G., 2015. Dirigent protein-mediated lignan and cyanogenic glucoside formation in flax seed: integrated omics and MALDI mass spectrometry imaging. *J. Nat. Prod.* 78, 1231–1242.
- Dopstadt, J., Vens-Cappell, S., Neubauer, L., Tudzynski, P., Cramer, B., Dreisewerd, K., Humpf, H.U., 2017. Localization of ergot alkaloids in sclerotia of *Claviceps purpurea* by matrix-assisted laser desorption/ionization mass spectrometry imaging. *Anal. Bioanal. Chem.* 409, 1221–1230.
- Dueñas, M.E., Klein, A.T., Alexander, L.E., Yandea-Nelson, M.D., Nikolau, B.J., Lee, Y.J., 2017. High spatial resolution mass spectrometry imaging reveals the genetically programmed, developmental modification of the distribution of thylakoid membrane lipids among individual cells of maize leaf. *Plant J.* 89, 825–838.
- Dug e de Bernonville, T., Clastre, M., Besseau, S.B., Oudin, A., Burlat, V., Gl evarec, G.L., Lanoue, A., Papon, N., Giglioli-Guivarc'h, N., St-Pierre, B., Courdavault, V., 2015. Phytochemical genomics of the Madagascar periwinkle: unravelling the last twists of the alkaloid engine. *Phytochemistry* 113, 9–23.
- El-Sayed, M., Verpoorte, R., 2007. *Catharanthus* terpenoid indole alkaloids: biosynthesis and regulation. *Phytochemistry Rev.* 6, 277–305.
- Faisal, M., Ahmad, N., Anis, M., 2005. Shoot multiplication in *Rauwolfia tetraphylla* L. using thidiazuron. *Plant Cell Tissue Organ Cult.* 80, 187–190.
- Gupta, S., Khanna, V.K., Maurya, A., Bawankule, D.U., Shukla, R.K., Pal, A., Srivastava, S.K., 2012. Bioactivity guided isolation of antipsychotic constituents from the leaves of *Rauwolfia tetraphylla* L. *Fitoterapia* 83, 1092–1099.
- Hagel, J.M., Yeung, E.C., Facchini, P.J., 2008. Got milk? The secret life of laticifers. *Trends Plant Sci.* 13, 631–639.
- Hammer, Ø., Harper, D.A.T., Ryan, P.D., 2001. PAST: paleontological statistics software package for education and data analysis. *Palaeontol. Electron.* 4 9pp.
- Hansen, A.C., Glassmire, A.E., Dyer, L.A., Smlanich, A.M., 2016. Patterns in parasitism frequency explained by diet and immunity. *Ecography* 40, 803–805.
- Hemalatha, R.G., Pradeep, T., 2013. Understanding the molecular signatures in leaves and flowers by desorption electrospray ionization mass spectrometry (DESI MS) imaging. *J. Agric. Food Chem.* 61, 7477–7487.
- Heskes, A.M., Sundram, T.C.M., Boughton, A., B.A. Jensen, N.B., Hansen, N.L., Crocoll, C., Cozzi, F., Rasmussen, S., Hamberger, B., Hamberger, B., Staerk, D., Moller, B.L., Pateraki, I., 2018. Biosynthesis of bioactive diterpenoids in the medicinal plant *Vitex*

- agnus-castus*. Plant J. 93, 943–958.
- Ifa, D.R., Srimany, A., Eberlin, L.S., Naik, H.R., Bhat, V., Cooks, R.G., Pradeep, T., 2011. Tissue imprint imaging by desorption electrospray ionization mass spectrometry. Anal. Methods 3, 1910–1912.
- Jiang, X., Liu, Y., Li, W., Zhao, L., Meng, F., Wang, Y., Tan, H., Yang, H., Wei, C., Wan, X., Gao, L., Xia, T., 2013. Tissue-Specific, Development-Dependent Phenolic Compounds Accumulation Profile and Gene Expression Pattern in Tea Plant *Camellia sinensis*. PLoS One 8, e62315.
- Kaushik, N., Kaushik, N., Attri, P., Kumar, N., Kim, C., Verma, A., Choi, E., 2013. Biomedical importance of indoles. Molecules 18, 6620.
- Kiesecker, C., Zitron, E., Lück, S., Bloehs, R., Scholz, E.P., Kathöfer, S., Thomas, D., Kreye, V.A.W., Katus, H.A., Schoels, W., Karle, C.A., Kiehn, J., 2004. Class Ia anti-arrhythmic drug ajmaline blocks HERG potassium channels: mode of action. Naunyn-Schmiedeberg's Arch. Pharmacol. 370, 423–435.
- Korte, A.R., Song, Z., Nikolau, B.J., Lee, Y.J., 2012. Mass spectrometric imaging as a high-spatial resolution tool for functional genomics: tissue-specific gene expression of TT7 inferred from heterogeneous distribution of metabolites in Arabidopsis flowers. Anal. Methods 4, 474–481.
- Kueger, S., Steinhäuser, D., Willmitzer, L., Giavalisco, P., 2012. High-resolution plant metabolomics: from mass spectral features to metabolites and from whole-cell analysis to subcellular metabolite distributions. Plant J. 70, 39–50.
- Lee, Y.J., Perdian, D.C., Song, Z., Yeung, E.S., Nikolau, B.J., 2012. Use of mass spectrometry for imaging metabolites in plants. Plant J. 70, 81–95.
- Liu, J., Cai, J., Wang, R., Yang, S., 2017. Transcriptional regulation and transport of terpenoid indole alkaloid in *Catharanthus roseus*: exploration of new research directions. Int. J. Mol. Sci. 18, 53.
- Mahata, M., Mahata, S.K., Parmer, R.J., O'Connor, D.T., 1996. Vesicular monoamine transport inhibitors. novel action at calcium channels to prevent catecholamine secretion hypertension. 28, 414–420.
- Mahroug, S., Courdavault, V., Thiersault, M., St-Pierre, B., Burlat, V., 2006. Epidermis is a pivotal site of at least four secondary metabolic pathways in *Catharanthus roseus* aerial organs. Planta 223, 1191–1200.
- Miettinen, K., Dong, L., Navrot, N., Schneider, T., Burlat, V., Pollier, J., Woittiez, L., van der Krol, S., Lugan, R.L., Ilc, T., Verpoorte, R., Oksman-Caldentey, K.M., Martinoia, E., Bouwmeester, H., Goossens, A., Memelink, J., Werck-Reichhart, D.L., 2014. The secoiridoid pathway from *Catharanthus roseus*. Nat. Commun. 5, 3606.
- Mohana Kumara, P., Srimany, A., Ravikanth, G., Uma Shaanker, R., Pradeep, T., 2015. Ambient ionization mass spectrometry imaging of rohitukine, a chromone anti-cancer alkaloid, during seed development in *Dysoxylum binectariferum* Hook.f (Meliaceae). Phytochemistry 116, 104–110.
- Mohana Kumara, P., Srimany, A., Arunan, S., Ravikanth, G., Uma Shaanker, R., Pradeep, T., 2016. Desorption Electrospray Ionization (DESI) Mass Spectrometric Imaging of the Distribution of Rohitukine in the Seedling of *Dysoxylum binectariferum* Hook. F. PLoS One 11 (6), e0158099.
- Nielsen, L.J., Stuart, P., Pičmanová, M., Rasmussen, S., Olsen, C.E., Harholt, J., Møller, B.L., Bjarnholt, N., 2016. Dhurrin metabolism in the developing grain of *Sorghum bicolor* (L.) Moench investigated by metabolite profiling and novel clustering analyses of time-resolved transcriptomic data. BMC Genomics 17, 1021.
- O'Connor, S.E., Maresh, J.J., 2006. Chemistry and biology of monoterpene indole alkaloid biosynthesis. Nat. Prod. Rep. 23, 532–547.
- Pan, Q., Mustafa, N.R., Tang, K., Choi, Y.H., Verpoorte, R., 2015. Monoterpenoid indole alkaloids biosynthesis and its regulation in *Catharanthus roseus*: a literature review from genes to metabolites. Phytochemistry Rev. 15, 221–250.
- Pandey, A., Swarnkar, V., Pandey, T., Srivastava, P., Kanojia, S., Mishra, D.K., Tripathi, V., 2016. Transcriptome and Metabolite analysis reveal candidate genes of the cardiac glycoside biosynthetic pathway from *Calotropis procera*. Sci. Rep. 6, 34464.
- Pathania, S., Acharya, V., 2016. Computational analysis of “-omics” data to identify transcription factors regulating secondary metabolism in *Rauvolfia serpentina*. Plant Mol. Biol. Rep. 34, 283–302.
- Schluttenhofer, C., Pattanaik, S., Patra, B., Yuan, L., 2014. Analyses of *Catharanthus roseus* and Arabidopsis thaliana WRKY transcription factors reveal involvement in jasmonate signaling. BMC Genomics 15, 502.
- Smith, C.A., I'Maille, G., Want, E.J., Qin, C., Trauger, S.A., Brandon, T.R., Custodio, D.E., Abagyan, R., Siuzdak, G., 2005. METLIN: a metabolite mass spectral database. Ther. Drug Monit. 27, 747–751.
- St-Pierre, B., Vazquez-Flota, F.A., De Luca, V., 1999. Multicellular compartmentation of *catharanthus roseus* alkaloid biosynthesis predicts intercellular translocation of a pathway intermediate. Plant Cell 11, 887–900.
- Sturtevant, D., Dueñas, M.E., Lee, Y.J., Chapman, K.D., 2017. Three-dimensional visualization of membrane phospholipid distributions in Arabidopsis thaliana seeds: a spatial perspective of molecular heterogeneity. BBA. Mol. Cell Biol. Lipids 1862, 268–281.
- Woodfield, H.K., Sturtevant, D., Borisjuk, L., Munz, E., Guschina, I.A., Chapman, K., Harwood, J.L., 2017. Spatial and temporal mapping of key lipid species in *Brassica napus* seeds. Plant Physiol. 173, 1998–2009.
- Yamamoto, K., Takahashi, K., Mizuno, H., Anegawa, A., Ishizaki, K., Fukaki, H., Ohnishi, M., Yamazaki, M., Masujima, T., Mimura, T., 2016. Cell-specific localization of alkaloids in *Catharanthus roseus* stem tissue measured with Imaging MS and Single-cell MS. Proc. Natl. Acad. Sci. U. S. A. 113, 3891–3896.
- Yu, F., De Luca, V., 2013. ATP-binding cassette transporter controls leaf surface secretion of anticancer drug components in *Catharanthus roseus*. Proc. Natl. Acad. Sci. U. S. A. 110, 15830–15835.
- Zhu, J., Wang, M., Wen, W., Yu, R., 2015. Biosynthesis and regulation of terpenoid indole alkaloids in *Catharanthus roseus*. Phcog. Rev. 9 (17), 24–28.
- Zifkin, M., Jin, A., Ozga, J.A., Zaharia, L.I., Scherthaner, J.P., Gesell, A., Abrams, S.R., Kennedy, J.A., Constabel, C.P., 2012. Gene expression and metabolite profiling of developing highbush blueberry fruit indicates transcriptional regulation of flavonoid metabolism and activation of abscisic acid metabolism. Plant Physiol. 158, 200–224.